Mechanisms of impaired pancreatic β-cell function in high-fat diet-induced obese mice: The role of endoplasmic reticulum stress

XIAOQING YI, XUAN CAI, SISI WANG and YANFENG XIAO

Department of Pediatrics, Second Affiliated Hospital of Xi'an Jiaotong University, Xi'an, Shaanxi 710004, P.R. China

Abstract. The aim of the study was to examine whether there was excessive endoplasmic reticulum stress (ERs) in the islets of high-fat diet (HFD)-induced obese mice, as well as the effects of ERs on β-cell function. Male C57BL/6J mice were fed a HFD for 16 weeks. Pancreatic β-cell function was evaluated using intraperitoneal glucose tolerance and insulin release tests, and via electron microscopy. The expression of activating transcription factor 6 (ATF6) and phosphorylated (p)-eukaryotic initiation factor 2α (eIF2α) were detected via immunofluorescence staining to determine whether exposure to a HFD induced ERs in pancreatic islets. *In vitro*, ERs was induced by palmitate (PA) in INS-1 cells, and the protein expression of ATF6, and mRNA expression of ATF6 and insulin were examined via western blot and quantitative PCR (qPCR) analyses, respectively. The nuclear localization of ATF6 was examined by immunofluorescence. Finally, small interfering (si)RNA was used to downregulate ATF6 expression in INS-1 cells to further determine whether ATF6 mediated the ERs-induced impairment of insulin gene transcription. After 16 weeks of induction, the obese mice showed impaired glucose tolerance, insulin resistance and hyperinsulinemia. Immunohistochemistry staining showed increased p-eIF2α and ATF6 expression in pancreatic islets in the obesity group compared with the normal group. Electron microscopy indicated that the microstructures and secretory functions of β-cells were impaired. After 24 h of incubation, ATF mRNA and protein expression in the PA group was significantly higher compared with the control group. However, the insulin mRNA expression in the PA group was significantly decreased. Furthermore, qPCR showed that the insulin mRNA expression was significantly increased 24 h after PA treatment in cells transfected with ATF6-siRNA compared with the negative control group. The present suggested shows that ERs-induced activation of ATF6 may play an important role in the development of β-cell dysfunction in obese mice.

Introduction

The mechanisms underlying the high prevalence of type 2 diabetes mellitus (T2DM) among obese individuals remain unclear (1). Insulin resistance and islet β-cell dysfunction are currently regarded as two key pathogenic mechanisms in the progression of obesity to diabetes (2). When various factors lead to insulin resistance in obese patients, β-cells compensate by increasing insulin secretion to maintain a normal blood glucose level and glucose tolerance; however, when the amount of insulin produced by β-cells is insufficient to compensate for the reduced insulin sensitivity of tissues, glucose homeostasis is disrupted, leading to impaired glucose tolerance and ultimately, diabetes (3).

The highly developed endoplasmic reticulum (ER) is an important feature of pancreatic β-cells that participates in multiple cellular biological functions, including insulin synthesis, post-translational modification and maintenance of intracellular calcium homeostasis (4). A number of patho-logical and physiological factors can influence ER function and disrupt ER homeostasis to induce ER stress (ERs), such as viral toxins, inflammatory cytokines, mutations and misfolded protein expression (5). Pancreatic β-cells are one of the cell types most sensitive to ERs. Under physiological conditions, moderate ERs contributes to the regulation of the synthesis and secretion of insulin by pancreatic β-cells, and helps maintain glucose homeostasis in the body (6). However, excessive long-term ERs results in toxic effects, leading to pancreatic β-cell dysfunction (7). A previous study on obesity has indicated that ERs is an integral component of obesity, insulin resistance and T2DM at the molecular, cellular and tissue levels (8). Excessive ERs is present in the peripheral tissues of patients with obesity, such as liver, muscle and adipose tissues (9). ERs blocks the insulin signaling pathway, leading to insulin resistance. However, it remains unclear whether excessive ERs also exists in the pancreatic tissues of individuals with obesity and leads to impaired islet β-cell functions.

Correspondence to: Dr Yanfeng Xiao, Department of Pediatrics, Second Affiliated Hospital of Xi'an Jiaotong University, 157 West Fifth Road, Xi'an, Shaanxi 710004, P.R. China
E-mail: caixuanqsc@foxmail.com

Following ERs development, the accumulation of a large amount of proteins in the ER lumen induces the downstream unfolded protein response (UPR) signaling pathway (10). ERs-induced UPR can selectively activate three signal transduction pathways in cells; a number of studies have indicated that activation of the protein kinase RNA-like ER kinase (PERK) and inositol-requiring enzyme 1α (IRE1α) signaling pathways plays important roles in the pathogenetic mechanisms underlying β-cell dysfunction (4,11). However, little is known concerning the influence of activating transcription factor 6 (ATF6) on β-cell functions. It has been demonstrated that ERs-inducing factors, such as hypoxia, tunicamycin and thapsigargin, can upregulate the expression of ATF6 mRNA, indicating that the increase in ATF6 expression is important for ERs responses and that ATF6 may serve a role in the development of cell dysfunction, similar to IRE1 and PERK (12).

In the present study, it was investigated as to whether there was an excessive ERs in the islets of high-fat diet (HFD)-induced obese mice, and the effects of ERs on β-cell function were evaluated. Subsequently, it was determined if high concentrations of palmitate (PA) induced ERs in cultured INS-1 cells, and whether ERs impaired insulin gene transcription. Finally, whether ERs-impaired insulin gene transcription was mediated by ATF6 was evaluated.

Materials and methods

HFD-induced obese mice. In total, 36 C57BL/6J mice (male; 3 weeks old; starting weight, 8.5-10 g) were obtained from Xi'an Jiaotong University Animal Center. The mice were housed in individual cages. Mice were provided with access to food and water *ad libitum*, and the temperature was controlled at 26-28°C. The relative humidity was 40-60%, and a 10:14 h light:dark cycle was maintained every day. After adaptive feeding with a normal diet for 1 week, the mice were randomly divided into a normal diet group and a HFD group (18 mice/group) and then fed with general feed or high-fat feed for 16 weeks. On caloric basis, the HFD consisted of 40% fat from lard, 41.8% carbohydrate, and 18.2% protein, whereas the normal diet contained 13.8% fat, 60.5% carbohydrate, and 25.7% protein. The body weight was measured once per week at a fixed time.

The study was approved by the Animal Ethics Committee at Xi'an Jiaotong University (permit no. 2017-30). The study was conducted in strict accordance with the recommendations of the Guide for the Care and Use of Laboratory Animals of the National Institutes of Health and the AVMA Guidelines for the Euthanasia of Animals 2013 Edition (13,14).

Intraperitoneal glucose tolerance test (IPGTT) and insulin release test. After 16 weeks, the mice were fasted for 15 h and subjected to an intraperitoneal injection of 25% glucose at 2 g/kg body weight. The blood glucose levels in the tail vein were measured before injection and at 30, 60 and 120 min after injection using a blood glucose meter. Venous blood samples (0.1 ml/sample) were collected from the retro-orbital venous plexus before injection and at 30, 60 and 120 min after injection. All animals were anesthetized with sodium pentobarbital (40 mg/kg, intraperitoneal) for retro-orbital sampling of blood.

The blood samples were centrifuged for 15 min at 1,000 x g at 4°C, and then serum samples were collected and stored at -70°C. ELISA was used for insulin detection (Mouse Insulin ELISA kit; cat. no. F6301; Westang Biological Technology Co., Ltd.).

Immunohistochemical analysis. To determine whether exposure to HFD induced excessive ERs in pancreatic islets, the expression levels of ATF6 and phosphorylated (p)-eukaryotic initiation factor 2α (eIF2α) were detected via immunofluorescence staining. ATF6 has two subtypes, ATF6α and ATF6β, with ATF6α playing more of a important role in the signaling pathway during endoplasmic reticulum stress (12). Therefore, ATF6α was investigated in the subsequent experiments. At the end of the tolerance test, mice were euthanized with an overdose of sodium pentobarbital (100 mg/kg, intraperitoneal), and pancreases were then dissected and frozen in liquid nitrogen (-196°C). Euthanasia was confirmed before disposal of all animal remains. A combination of criteria were used in confirming death, including lack of pulse, breathing, corneal reflex and response to firm toe pinch, graying of the mucous membranes and rigor mortis. Pancreases were cut into cryostat sections (4-8 μm; -20°C) and embedded in cryomolds with Tissue-Tek® O.C.T.™ mounting medium (Sakura Finetek USA, Inc.). Pancreatic sections were permeabilized with Triton X-100/TBS and pre-incubated with 2% BSA (cat. no. C500626; Sangon Biotech Co., Ltd.) in PBS for 10 min at room temperature. The sections were incubated overnight at 4°C with rabbit anti-mouse p-eIF2α antibody (1:200; cat. no. 11279; Signalway Antibody LLC) or mouse monoclonal ATF6 antibody (1:100; cat. no. ab11909; Abcam). The sections were rinsed three times with PBS, and incubated for 1 h at 4°C with the secondary antibody, Cy3®-conjugated goat anti-rabbit or goat anti-mouse IgG antibody (1:100; cat. nos. BA1031 and BA1032; Boster Biological Technology). Following washing for three times, buffered glycerol was added dropwise onto the sections, which were then covered with coverslips. Staining was observed under a fluorescence microscope with the magnification of x20 (Leica Microsystems GmbH) and ten fields containing islets were randomly selected from each section. Images were analyzed using Leica Confocal software (version 2.61; Leica Microsystems GmbH).

Electron microscopy. Mice were sacrificed and pancreatic tissues were harvested as described above. Pancreatic samples were cut into small cubes (1 mm³), and immediately placed in a 2.5% glutaraldehyde fixative solution (containing 0.1 M PBS and 4% paraformaldehyde) at 4°C for >2 h. After rinsing with PBS, the samples were fixed in a 2% osmium tetroxide solution at 4°C for 2 h and and epoxy resin/propylene oxide 1:1 mixture for 1 h at 37°C. Samples were embedded in epoxy resin for 1 h at 37°C and polymerized at 60°C overnight for ultra-thin sectioning (thickness, 100 nm). The samples were stained with uranyl acetate and lead citrate at room temperature for 30 min. Sections were examined under a H-600 transmission electron microscope (Hitachi, Ltd.) at 80 kV.

Cell culture. The INS-1 rat insulinoma cell line (Biohermes Biomedical Technology Co., Ltd.) was cultured in 5% CO_2-95% air at 37°C in RPMI-1640 medium (cat. no. 22400071; Thermo

Fisher Scientific, Inc.) containing 11.1 mM glucose and 2 mM l-glutamine. The medium was supplemented with 10% FBS (cat. no. SV30087; Thermo Fisher Scientific, Inc.), 1 mM pyruvate, 10 mM HEPES, 0.05 mM 2-mercaptoethanol, 100 U/ml penicillin and 100 mg/ml streptomycin. All experiments were performed using INS-1 cells between their 20 and 30th passages. Preparation of culture media containing PA (cat. no. P9767; Sigma-Aldrich; Merck KGaA) was performed as follows: The concentration of PA was 0.5 mM, and the final fatty acid-free BSA concentration was 0.1 mM. Therefore, the molar ratio of PA:BSA ranged between 1:1 and 5:1. All control conditions contained the same quantities of BSA as those with PA. The normal control group contained RPMI-1640 medium with 10% FBS. The BSA control group contained RPMI-1640 medium with 0.5% BSA, and the PA treatment group contained RPMI-1640 medium with 0.5 mM PA and 0.5% BSA.

Western blot analysis. INS-1 cells were plated into 6-well plates (10^6 cells/well) and cultured at 37°C for 48 h in RPMI-1640, followed by further culture in the same medium containing 0.5 mM PA for 24 h. Cells were collected following PA treatment and lysed using RIPA protein lysis buffer on ice (cat. no. R0020; Beijing Solarbio Science and Technology Co., Ltd.). Samples were centrifuged at 4°C and 12,000 x g for 10 min. Supernatants were collected and aliquoted. The Bradford protein assay kit (cat. no. 23200; Thermo Fisher Scientific, Inc.)was used for protein quantitation. Next, 4X sample buffer was added, and the samples were heated at 100°C for 10 min to denature proteins for SDS-PAGE (protein sample, 50 μg/lane; 8% SDS). The proteins were transferred onto a PVDF membrane and blocked in 5% skimmed milk for 2 h at room temperature. The membrane was incubated with the anti-ATF6 antibody (1:100; cat. no. ab11909; Abcam) at 4°C overnight. The membrane was then washed with TBS-Tween 20 (0.1% Tween 20) and incubated with horseradish peroxidase-conjugated secondary antibodies (1:100; cat. nos. ZB2301 and ZB2305; Beijing Zhongshan Golden Bridge Biotechnology Co., Ltd; OriGene Technologies, Inc.) at 4°C for 2 h. Protein bands were visualized using an enhanced chemiluminescence kit (cat. no. 32132X3; Thermo Fisher Scientific, Inc.). GAPDH (1:1,000; cat. no. TA-08; Beijing Zhongshan Golden Bridge Biotechnology Co., Ltd.) was used as the internal control. The gray density values were scanned, and the relative protein expression levels were analyzed using Gel-Pro-Analyzer software 4.0 (Media Cybernetics, Inc.).

Reverse transcription-quantitative PCR (RT-qPCR). For RT-qPCR, total RNA was isolated from INS-1 cells using TRIzol® reagent (Invitrogen; Thermo Fisher Scientific, Inc.). cDNA was synthesized using a PrimeScript® RT Master Mix kit (Takara Bio, Inc.), according to the manufacturer's protocols. The resulting cDNA was used for qPCR analysis using an SYBR® Premix Ex Taq™ II system (Takara Bio, Inc.). For PCR amplification the following protocol was used: 95°C for 30 sec, followed by 40 cycles of 95°C for 5 sec and 60°C for 30 sec. qPCR was performed in a Bio-Rad IQ5 system (Bio-Rad Laboratories, Inc.). The following primers were used: ATF6, forward 5'-ACAAGACCGAAGATGTCCATTGTG-3', reverse 5'-GATCCTGGTGTCCATGACCTGA-3'; insulin, forward 5'-CAGCACCTTTGTGGTTCTCACTT-3', reverse 5'-CTC CACCCAGCTCCAGTTGT-3'; and GAPDH, forward 5'-GGC ACAGTCAAGGCTGAGAATG-3' and reverse 5'-ATGGTG GTGAAGACGCCAGTA-3'.

The amplified products were analyzed by agarose gel electrophoresis (2% agarose) to validate qPCR analysis. Ethidium bromide (cat. no. E1385; Sigma-Aldrich; Merck KGaA) was used for visualization. The standard curve and corresponding values for each sample were determined using the Bio-Rad IQ5 system. GAPDH was used as the internal control, and the $2^{-\Delta\Delta Cq}$ method was used to calculate the relative expression levels of the target genes (15).

Immunofluorescence analysis (nuclear localization of ATF6). Cells were plated on cover glasses before incubating them for 48 h in the standard culture medium described in the '*Cell culture*' section. After cultivation for 24 h in media containing 0.5 mM PA, the cells were fixed in 4% paraformaldehyde at room temperature for 20 min and permeabilized in Triton X-100 at room temperature for 30 min. The cells were pre-incubated with 2% BSA (cat. no. C500626; Sangon Biotech Co., Ltd.) for 10 min at room temperature. Then the cells were incubated with ATF6 antibody overnight at 4°C (1:100; cat. no. ab11909; Abcam) and subsequently the Cy3®-conjugated secondary antibody 1 h at 4°C (1:100; cat. no. BA1031, Boster Biological Technology). The nuclei were stained with DAPI for 15 min at room temperature, and the samples were mounted in glycerol and observed under a fluorescence microscope with the magnification of x40.

Small interfering (si)RNA transfection for ATF6. ATF6-specific siRNAs were synthesized by Samchully Pharm Co., Ltd. and Bioneer Corporation. Three candidate ATF6-siRNAs were synthesized and evaluated for their ATF6 knockdown efficiency prior to the formal experiment. The candidate siRNAs were transfected into INS-1 cells and the expression of ATF6 was detected via RT-qPCR after 24 h of transfection. ATF6-siRNA2 had the greatest impact on ATF6 expression and was selected for subsequent experiments. The sequences of ATF6-siRNA and the nonspecific control siRNA (con-siRNA) were as follows: ATF6-siRNA1, 5'-GCAGUCGAUUAUCAGUAUATT-3' (sense); ATF6-siRNA2, 5'-CUGGGUUCAUAGACAUGA ATT-3' (sense); ATF6-siRNA3, 5'-GGGCAGGAUUAUGAA GUAATT-3' (sense); con-siRNA, 5'-UUCUCCGAACGUGUC ACGUTT-3' (sense). Transfections were performed according to the manufacturer's protocols. Briefly, INS-1 cells were plated into 6-well plates (10^6 cells/well) and cultured for 48 h in RPMI-1640. Lipofectamine® 2000 (Invitrogen; Thermo Fisher Scientific, Inc.) was diluted and mixed with ATF-siRNA. The mixture (containing 100 nmol/l siRNA) was added to the plates. After 6 h of transfection, transfection was evaluated by observing the uptake of fluorescein-tagged siRNA (FAM-siRNA) by the cells under a fluorescence microscope with a magnification of x20. Following successful transfection, the culture medium was replaced with lipophilic medium containing 0.5 mM PA for continuous culture for 24 h. RNA was extracted for RT-qPCR analysis to detect changes in the expression of insulin mRNA.

Statistical analysis. Data are presented as the mean ± SE of at least three independent experiments. Statistical analysis was performed using one-way ANOVA and two-way ANOVA.
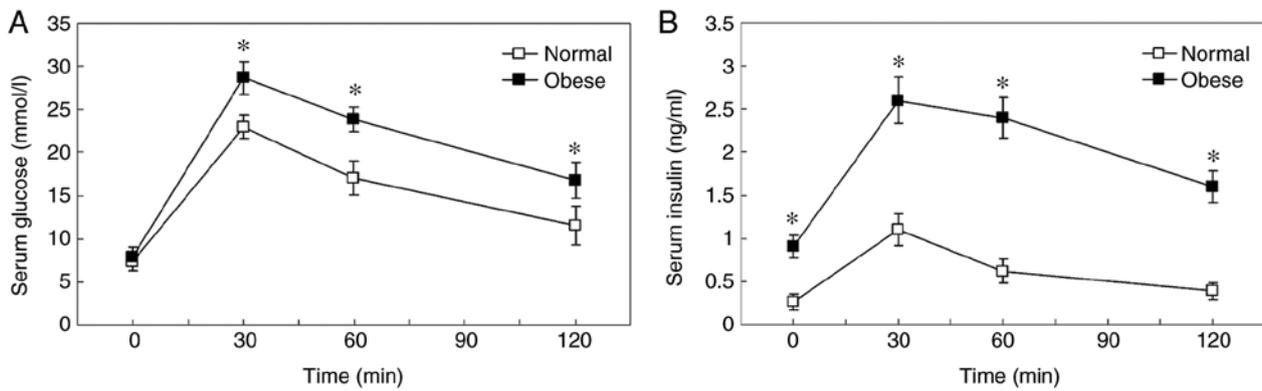
Figure 1. IPGTT and insulin release test. (A) IPGTT. (B) Insulin release test. *P<0.05 vs. normal. IPGTT, intraperitoneal glucose tolerance test.

Post hoc analysis was performed using Bonferroni correction for multiple comparisons. P<0.05 was considered to indicate a statistically significant difference.

Results

Obese mouse model. The body weights of the HFD-fed mice were similar to those of the normal diet-fed mice at the beginning of the experiment (data not shown). During the first week after the introduction of the HFD, a significantly greater increase in the body weights of the HFD-fed mice was observed compared with the normal diet-fed mice (P=0.009). The significant increase in the body weight gain of the HFD-fed mice relative to the normal diet control group was maintained until the end of the study. After 16 weeks' induction, mice fed with HFD had 24% higher body weights (37.4±3.8 g) compared with the normal group (29.8±2.4 g; P=0.0004), and developed adiposity with excessive adipose tissue pad mass. Thus, it was determined that the obese model was successfully established.

IPGTT and insulin release test. Basal plasma glucose levels of the obese mice were similar to the normal control. Following an intraperitoneal injection of glucose, the concentration of glucose in the blood increased to a maximum at 30 min in the two groups (Fig. 1). Blood glucose levels were notably higher at 30, 60 and 120 min in obese mice compared with normal mice, which indicated impaired glucose tolerance (Fig. 1A; P=0.0003 at 30 min; P=0.0006 at 60 min; P=0.0015 at 120 min). In addition, the HFD-induced obese mice exhibited ~3-fold higher fasting plasma insulin levels compared with the control groups at the beginning of the study (P=0.004). Following intraperitoneal injection of glucose, insulin levels were significantly higher in obese mice compared with normal control mice at all time points, indicating insulin resistance (Fig. 1B; P=0.0240 at 30 min; P=0.0008 at 60 min; P=0.0020 at 120 min;). Plasma insulin levels increased to a maximum at 30 min in the two groups. Compared with the baseline, insulin levels of the obese mice increased 3-fold at 30 min, wherever those of the controls increased 5-fold, which suggested decreased compensatory insulin secretory ability in HFD mice.

ERs status in the pancreas of obese mice. Immunohistochemical staining results showed increased p-eIF2α expression in pancreatic islets in the obese group compared with the normal group (Fig. 2; P=0.0071). In addition, ATF6 staining intensity was significantly increased in the pancreatic islets of obese mice (Fig. 2; P=0.0115). These results suggested that the pancreatic islets of obese mice had undergone excessive ERs and that the ATF6 signaling pathway was activated. Electron microscopy revealed the following results in pancreatic β-cells from obese mice (Fig. 3): Chromatin was slightly condensed in the nucleus; perinuclear spaces were widened; Golgi complex cisternae were dilated; the rough ER was dilated and degranulated; dilated cisternae contained low-electron density substances; mitochondria were swollen; mitochondria volume was increased; endocrine particles in the cytoplasm decreased; and endocrine particle volume increased. These results revealed that the pancreatic islet β-cells of obese mice exhibted changes in ER microstructures. In addition, the reduction of insulin secretory granules also suggested that the secretory function of β-cells was impaired.

PA-induced ERs in INS-1 cells. To confirm whether the high-lipid environment induced β-cell ERs, INS-1 cells were cultured in a high-lipid environment, and the expression of ATF6 protein in cells was measured via western blot analysis (Fig. 4). The expression level of ATF6 protein in the BSA control group was not significantly different compared with that of the normal control group. However, in the presence of 0.5 mM PA, ATF6 expression increased significantly following 24 h exposure, which suggested that prolonged exposure to PA may induce ERs.

PA treatment induces nuclear localization of ATF6. Immunofluorescence staining showed that ATF6 (Fig. 5; red) was expressed at low levels in the cytoplasm of INS-1 cells in the BSA control group, and that there was no ATF6 expression in the nucleus (Fig. 5). After the cells were treated with 0.5 mM PA, ATF6 was expressed in both the cytoplasm and the nucleus, and the expression levels were markedly higher compared with those in the BSA control group. These results suggested that PA treatment induced nuclear localization of ATF6 in INS-1 cells.

ERs in INS-1 cells impairs insulin gene expression. To confirm whether ERs influenced insulin gene expression, INS-1 cells were cultured in a high-lipid environment, and
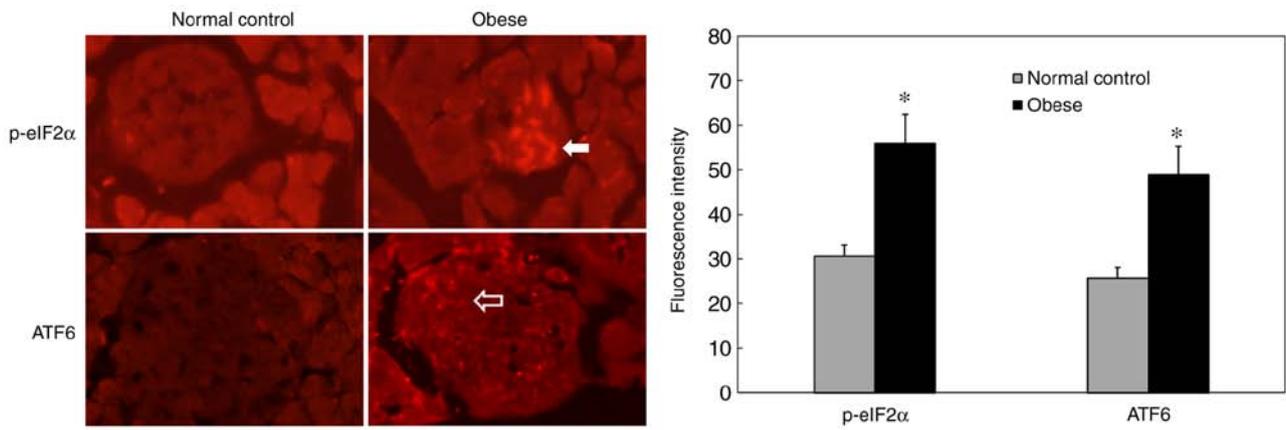
Figure 2. Immunofluorescence staining of ATF6 and p-eIF2α in pancreas islets. p-eIF2α (white arrow) and ATF6 (blank arrow) staining intensities were increased in pancreatic islets from the obese group compared with the normal control group. Magnification, x200. *P<0.05 vs. normal control. ATF6, activating transcription factor 6; eIF2α, eukaryotic initiation factor 2α; p, phosphorylated.
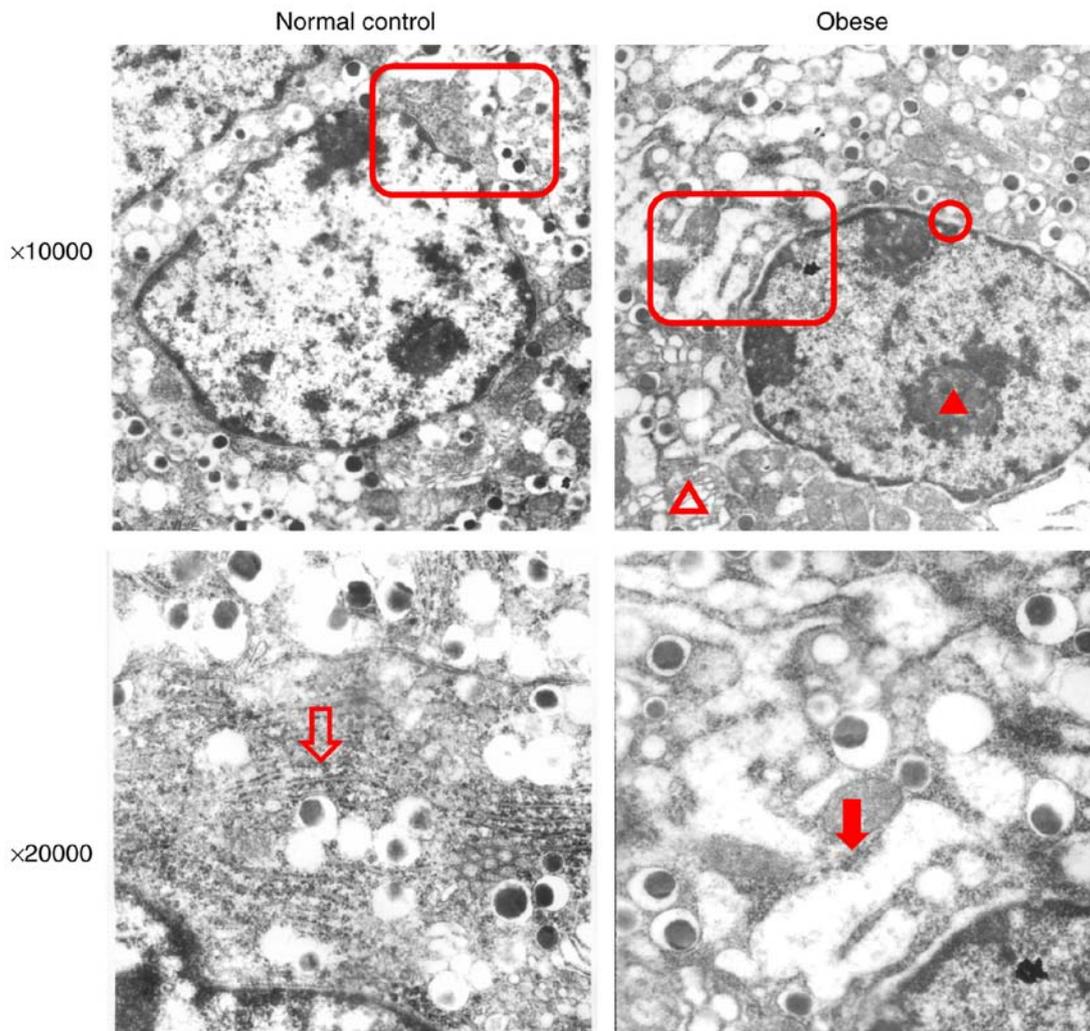

Figure 3. Electron microscopy of the microstructures of the ER in obese mice. The red blank triangles indicate the areas shown in the images below. Blank arrow: The normal rough ER in the normal group. Red arrow: Dilation, degranulation and vacuole-like changes of the rough ER in obese mice. Red triangle: Condensed chromatin in the nucleus. Blank red triangle: Swollen mitochondria. Red circle: Extended perinuclear space. ER, endoplasmic reticulum.

insulin mRNA expression levels were detected via RT-qPCR (Fig. 6). After 24 h of incubation, the expression level of ATF6 in the PA group was significantly higher compared with that in the BSA control group. In addition, the mRNA expression level of insulin in the normal control group was not significantly different compared with that in the BSA control
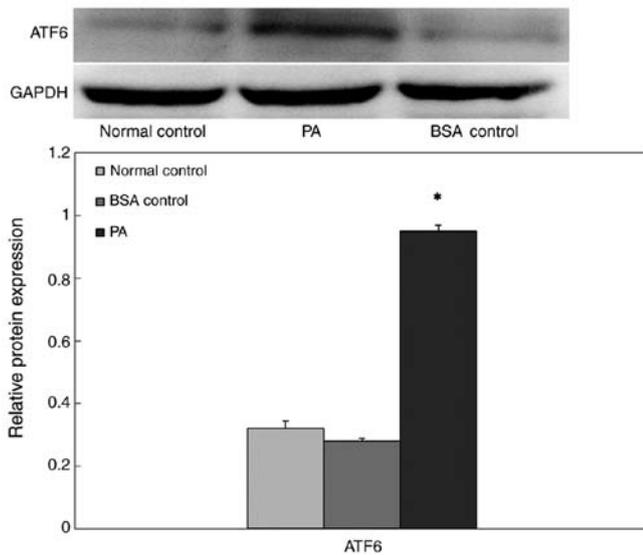
Figure 4. Western blot analysis of ATF6 expression in INS-1 cells cultured in a high-lipid environment. *P<0.05 vs. normal control group and BSA control group. ATF6, activating transcription factor 6; PA, palmitate.

group. The insulin mRNA expression level in the PA group was significantly decreased. These results suggested that PA inhibited insulin mRNA expression in INS-1 cells.

ERs-induced impairment of insulin gene transcription is mediated by ATF6. The inhibitory effects of three candidate siRNAs were evaluated. The results showed that ATF6-siRNA2 had the best inhibitory effect compared with other candidate siRNAs (Fig. 7). Therefore, subsequent experiments were performed using ATF6-siRNA2 to ensure that ATF6 was inhibited. To test whether ATF6 mediated the ERs-induced insulin gene transcription impairment, ATF6-siRNA2 was transfected into INS-1 cells which were subsequently cultured in a high-lipid environment for 24 h. RT-qPCR showed that the mRNA expression of insulin was significantly increased following a 24 h PA treatment in cells transfected with ATF6-siRNA2 compared with untransfected cells and cells transfected with con-siRNA (Fig. 8). Thus, ATF6 knockdown attenuated the inhibitory effect of PA on insulin mRNA expression.

Discussion

Obesity is associated with the activation of cellular stress signals (9); however, the origin of this stress is still not clear. One key component of cellular stress responses is the ER (16). Multiple pathological and physiological factors can disrupt ER homeostasis to cause ERs, including aging, viral infection, environmental toxins, inflammatory cytokines, glucose or nutritional deficiency, increased lipid and secretory protein synthesis, mutations and misfolded protein expression (17). A number of these factors are present in obesity. Ozcan *et al* (18) detected the expression levels of ERs-related indicators (p-PERK, p-eIF2α and glucose-regulated protein 78 kDa) in the peripheral tissues (liver, adipose tissue and muscle) of HFD-induced and genetic (*ob/ob*) models of obese mice. These results revealed increased expression levels of

ERs-related indicators in liver and adipose tissues, suggesting that obesity may induce excessive ERs. However, it remains unclear whether excessive ERs also exists in the pancreatic tissues of obese individuals and further compromises islet β-cell functions. In the present study, male C57BL/6J mice were used as the experimental subjects. After a 16 week induction, mice fed a HFD exhibited higher body weights compared with the normal diet group, and developed adiposity with excessive adipose tissue pad mass. The obese mice showed impaired glucose tolerance, insulin resistance and decreased ability of compensatory secretion of insulin. Furthermore, the microstructures of islet β-cells of obese mice were observed via transmission electron microscopy. Rough ER expansion and degranulation were observed, with low-electron density materials in the expanded lumen, suggesting the presence of excessive ERs. In addition, structural changes in other organelles in the nuclei and cytoplasm, such as the Golgi apparatus and mitochondria, were also observed, with reduced numbers of insulin secretory granules, suggesting a degree of impairment in the secretory functions of β-cells.

After ERs development, the accumulation of a large amount of proteins in the ER lumen induces the downstream UPR signaling pathway (19). UPR signaling is mediated by ERs signal transduction molecules, including PERK, IRE1α and ATF6, which are important transmembrane proteins in the ER (20). eIF2α is a key molecule in the PERK-mediated signaling pathway. The phosphorylation status of eIF2α is an important evaluation indicator of ERs (4). Gregor *et al* (21) detected changes in eIF2α expression in the livers of obese patients using immunofluorescence staining when evaluating changes in the ERs status of patients before and after weight loss. The immunofluorescence staining results in the present study showed that p-eIF2α expression in the pancreatic islets of obese mice was significantly higher compared with in normal mice, suggesting that the pancreatic islets of obese mice had excessive ERs. ATF6 is an ER membrane-bound transcription factor; it is a member of the ATF/cAMP response element-binding protein basic-leucine zipper family of DNA-binding proteins (22). The present study detected the α subtype of ATF6, and the results showed that it was expressed in the pancreatic islets of both normal mice and obese mice, but at higher levels in the latter. These results further suggested that the pancreatic islets of HFD obese mice had ERs, and that the ATF6-mediated signal transduction pathway was activated.

Dyslipidemia is the most typical pathophysiological change in patients with obesity, of which hypertriglyceridemia is the major form (23). Triglycerides are hydrolyzed into free fatty acids (FFAs) by lipoprotein lipases; when the increase in FFAs in blood exceeds the storage capacity of adipose tissues and the oxidation ability of all tissues, excess FFAs are deposited in non-adipose tissues (24). Cell injury caused by an overly high FFA level combined with triglyceride accumulation is termed β-cell lipotoxicity, which is a potential factor causing cell dysfunction (25,26). However, the molecular mechanisms underlying FFA-mediated β-cell lipotoxicity are still not completely understood. Karaskov *et al* (27) treated β-cells with PA, a saturated fatty acid containing 16 carbon atoms that is an important component of vegetable and animal oils, for 16-24 h. Their results demonstrated that the levels
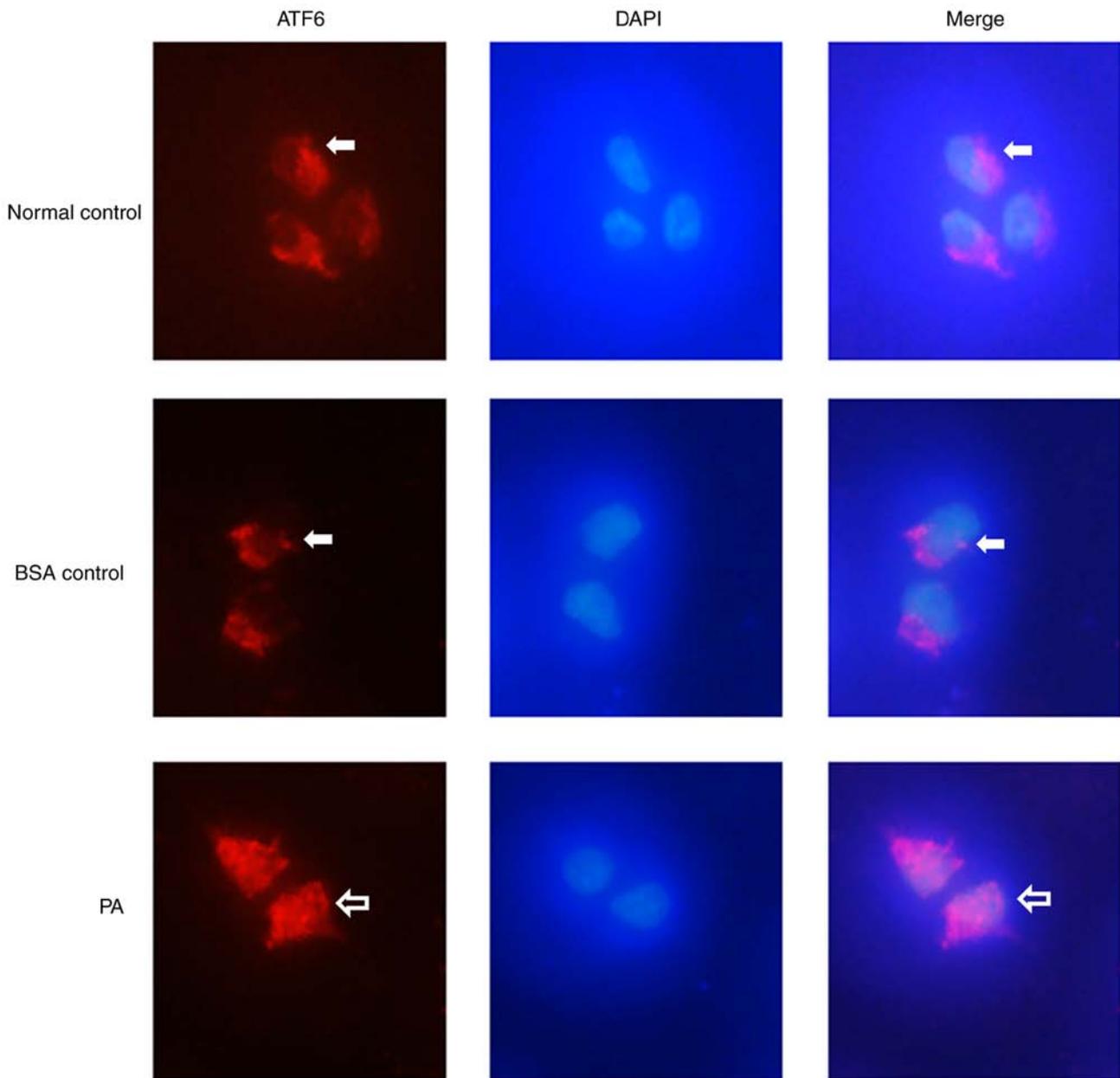
Figure 5. Nuclear localization of ATF6 in INS-1 cells after PA treatment. ATF6 was visualized in red, DAPI nuclear staining in blue. ATF6 (white arrows) localized to the cytoplasm of INS-1 cells in the control group, with no ATF6 expression in the nucleus. Treatment with 0.5 mM PA induced nuclear localization of ATF6 in INS-1 cells; ATF6 was expressed in both the cytoplasm and the nucleus (blank arrows). Magnification, x40. ATF6, activating transcription factor 6; PA, palmitate.

of p-eIF2α, ATF4 and X-box binding protein 1 were significantly increased, and that ER morphology and molecular chaperone distribution were significantly changed, indicating that PA induced ERs in β-cells, and activated the PERK and IRE1α signaling pathways. By contrast, treatment with oleate, which is an unsaturated fatty acid containing 18 carbon atoms and one double bond, did not induce ERs responses. However, whether PA can activate the ATF6 signaling pathway remains to be determined (28,29). In the present study, INS-1 cells were cultured in the presence of 0.5 mM PA, and the expression levels of ATF6 were analyzed via western blotting. To avoid the use of over-passaged cells to ensure reliable and reproducible results, INS-1 cells between their 20th and 30th passages were used. INS-1, a rat insulinoma cell line, was considered

the most reliable insulin-secreting β-cell line that is stable in morphology, responses to stimuli, growth rates, protein expression and transfection efficiency within 30 consecutive passages (30). Various studies involving the use of the INS-1 cell line for investigating stimulated insulin release have used cells between passages 20 and 30 (31-34). In addition, the capacity for insulin secretion of INS-1 cells between their 20 and 30th passages was confirmed by preliminary experiments prior to the reported experiments (data not shown). The present study demonstrated that in the presence of PA, ATF6 expression increased significantly in INS-1 cells. qPCR analysis also revealed that ATF6 expression increased under PA conditions. These results suggested that prolonged exposure to PA may induce ERs and activate the ATF6 pathway.
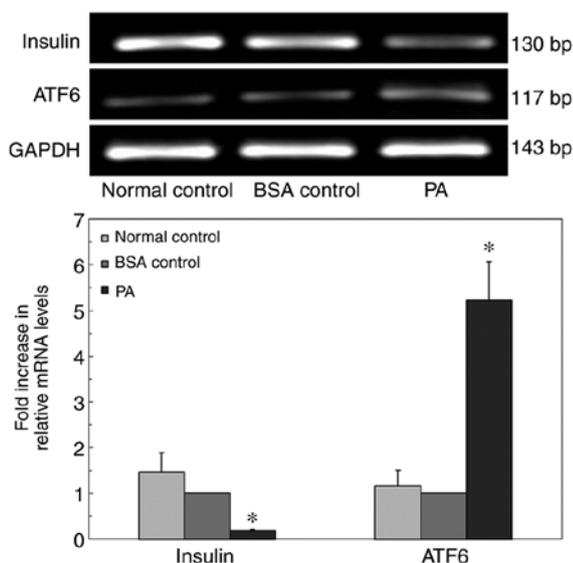
Figure 6. Quantitative PCR analysis of ATF6 and insulin mRNA expression in INS-1 cells cultured in a high-lipid environment. *P<0.05 vs. normal control group and BSA control group. ATF6, activating transcription factor 6; PA, palmitate.
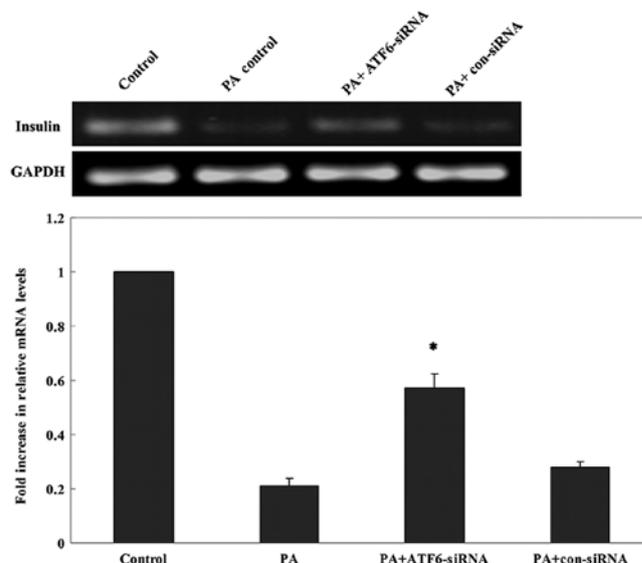

Figure 8. Quantitative PCR analysis of insulin mRNA expression 24 h after PA treatment in INS-1 cells transfected with ATF6-siRNA. *P<0.05 vs. PA group, PA+con-siRNA group and untransfected control group. ATF6, activating transcription factor 6; con, control; PA, palmitate; siRNA, small interfering RNA.
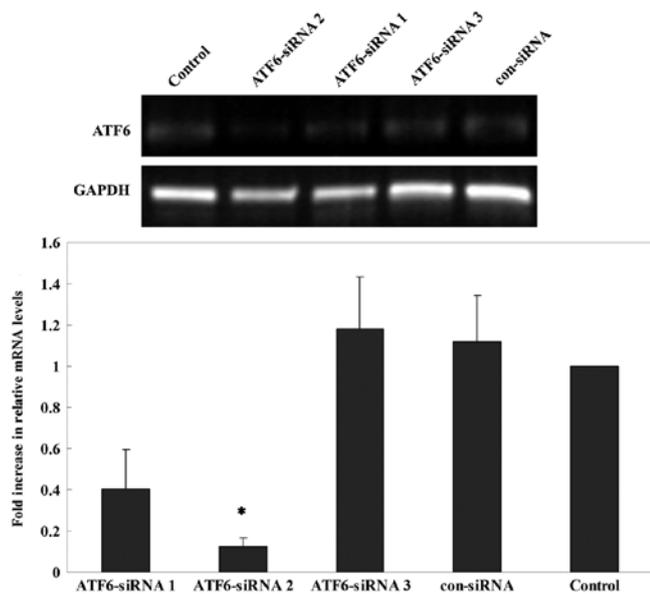

Figure 7. Inhibitory efficiency of three candidate siRNAs targeting ATF6. ATF6-siRNA2 had the greatest impact on ATF6 expression and was selected for subsequent experiments. *P<0.05 vs. siRNA groups, con-siRNA group and untransfected control group. ATF6, activating transcription factor 6; con, control; siRNA, small interfering RNA.

Under normal conditions, ATF6 interacts with the ER protein chaperone binding immunoglobulin protein/GRP78 and is retained in the ER membrane (35). During ERs, unfolded protein accumulation induces the transfer of ATF6 to the Golgi apparatus to be hydrolyzed into active fragments (22). Activated ATF6 enters the nucleus to activate the ERs response element on the promoter regions of several genes in order to promote the correct folding of proteins in the ER lumen (36). In the present study, immunofluorescence staining showed that in normal INS-1 cells, ATF6 was mainly expressed at a low level in the cytoplasm, with nearly no expression in the nucleus. However, in cells treated with PA, both cytoplasmic and nuclear ATF6 expression were observed, with higher expression levels than those observed in normal cells. These findings suggested that in INS-1 cells treated with PA, ATF6 protein was activated and translocated from the cytoplasm into the nuclei.

The most important function of β-cells is to synthesize and secrete insulin, which is generated via expression of the insulin gene. To determine whether signaling induced by long-term excessive ERs may affect insulin mRNA expression, the expression of insulin mRNA was examined via RT-qPCR in the present study. The results indicated that following the treatment of INS-1 cells with PA, insulin mRNA expression was significantly decreased compared with in uninduced cells, and the ATF6 signaling pathway was activated. These results suggested that ATF6 may serve an important role in ERs-induced cell dysfunction. Therefore, to further verify whether ATF6 mediated the ERs-induced impairment of insulin gene transcription, siRNA was used to knock down ATF6 expression in INS-1 cells in subsequent experiments; the results demonstrated that compared with untransfected cells, transfected cells cultured for 24 h with PA exhibited increased insulin mRNA expression. This result suggested that PA may inhibit insulin mRNA expression in β-cells by activating the ATF6 signaling pathway; downregulation of ATF6 may ameliorate the inhibitory effect of PA on insulin mRNA expression. Seo *et al* (34) obtained similar findings by transfecting ATF6-siRNA into INS-1 cells and culturing the cells in a high-glucose environment (30 mM glucose) for 48 h. It was also reported that northern blot analysis indicated significantly higher insulin mRNA expression levels in cells transfected with ATF6-siRNA compared with the untransfected group, and it was revealed that ATF6-siRNA significantly reversed the inhibition of insulin mRNA expression by high glucose. In addition, the results of the present

study were also consistent with the findings of Hong *et al* (37). Given these findings, ATF6 may play an important role in the impairment of β-cells under high-glucose and high-fat conditions. This conclusion also reflects the intrinsic links between obesity and T2DM.

The present study used HFD-induced obese mice to evaluate the ERs status in the pancreas of obese mice, and to evaluate the influence of obesity on glucose metabolism and pancreatic islet β-cell function in the body. Changes in ATF6, an important signaling molecule in the process of ERs in β-cells, at the protein and mRNA levels, and its influence on insulin mRNA expression in β-cells were investigated using *in vitro* experiments. The results confirmed that activation of the ATF6 signaling pathway induced by excessive ERs was one of the potential mechanisms underlying β-cell dysfunction in obesity. The present study theoretically elucidated potential mechanisms underlying the high prevalence of T2DM among obese patients, indicating novel strategies for effective prevention and control of the development of obesity-related T2DM in clinical practice.

Acknowledgements

Not applicable.

Funding

Availability of data and materials

The data set used and/or analyzed during the present study are available from the corresponding author on reasonable request.

Authors' contributions

XY conceived and coordinated the study, designed and performed the experiments, analyzed the data and drafted the manuscript. XC, SW and YX performed the data collection, analyzed the data and revised the manuscript. All authors reviewed the results and approved the final version of the manuscript.

Ethics approval and consent to participate

The study was approved by the Animal Ethics Committee at Xi'an Jiaotong University (permit no. 2017-30). The study was conducted in strict accordance with the recommendations of the Guide for the Care and Use of Laboratory Animals of the National Institutes of Health and the AVMA Guidelines for the Euthanasia of Animals 2013 Edition.

Patient consent for publication

Not applicable.

Competing interests

The authors declare that they have no competing interests.

References

1. Leitner DR, Frühbeck G, Yumuk V, Schindler K, Micic D, Woodward E and Toplak H: Obesity and type 2 diabetes: Two diseases with a need for combined treatment strategies - EASO can lead the way. Obes Facts 10: 483-492, 2017.
2. Kahn SE, Cooper ME and Del Prato S: Pathophysiology and treatment of type 2 diabetes: Perspectives on the past, present, and future. Lancet 383: 1068-1083, 2014.
3. Prieto D, Contreras C and Sanchez A: Endothelial dysfunction, obesity and insulin resistance. Curr Vas Pharmacol 12: 412-426, 2014.
4. Cnop M, Toivonen S, Igoillo-Esteve M and Salpea P: Endoplasmic reticulum stress and eIF2α phosphorylation: The achilles heel of pancreatic β cells. Mol Metab 6: 1024-1039, 2017.
5. Sun J, Cui J, He Q, Chen Z, Arvan P and Liu M: Proinsulin misfolding and endoplasmic reticulum stress during the development and progression of diabetes. Mol Aspects Med 42: 105-118, 2015.
6. Rabhi N, Salas E, Froguel P and Annicotte JS: Role of the unfolded protein response in β cell compensation and failure during diabetes. J Diabetes Res 2014: 795171, 2014.
7. Hu Y, Gao Y, Zhang M, Deng KY, Singh R, Tian Q, Gong Y, Pan Z, Liu Q, Boisclair YR and Long Q: Endoplasmic reticulum-associated degradation (ERAD) has a critical role in supporting glucose-stimulated insulin secretion in pancreatic β-cells. Diabetes 68: 733-746, 2019.
8. Sovolyova N, Healy S, Samali A and Logue SE: Stressed to death-mechanisms of ER stress-induced cell death. Biol Chem 395: 1-13, 2014.
9. Yilmaz E: Endoplasmic reticulum stress and obesity. Adv Exp Med Biol 960: 261-276, 2017.
10. Lee J and Ozcan U: Unfolded protein response signaling and metabolic diseases. J Biol Chem 289: 1203-1211, 2014.
11. Tsuchiya Y, Saito M and Kohno K: Pathogenic mechanism of diabetes development due to dysfunction of unfolded protein response. Yakugaku Zasshi 136: 817-825, 2016 (In Japanese).
12. Namba T, Ishihara T, Tanaka K, Hoshino T and Mizushima T: Transcriptional activation of ATF6 by endoplasmic reticulum stressors. Biochem Biophys Res Commun 355: 543-548, 2007.
13. National Research Council (US) Committee for the Update of the Guide for the Care and Use of Laboratory Animals. Guide for the Care and Use of Laboratory Animals; 2011.
14. AVMA Guidelines for the Euthanasia of Animals: 2013 Edition. Available at: https://www.avma.org/kb/policies/documents/euthanasia.pdf.
15. Livak KJ and Schmittgen TD: Analysis of relative gene expression data using real-time quantitative PCR and the 2(-Delta Delta C(T)) method. Methods 25: 402-408, 2001.
16. Esser N, Legrand-Poels S, Piette J, Scheen AJ and Paquot N: Inflammation as a link between obesity, metabolic syndrome and type 2 diabetes. Diab Res Clin Pract 105: 141-150, 2014.
17. Fonseca SG, Burcin M, Gromada J and Urano F: Endoplasmic reticulum stress in beta-cells and development of diabetes. Cur Opin Pharm 9: 763-770, 2009.
18. Ozcan U, Cao Q, Yilmaz E, Lee AH, Iwakoshi NN, Ozdelen E, Tuncman G, Görgün C, Glimcher LH and Hotamisligil GS: Endoplasmic reticulum stress links obesity, insulin action, and type 2 diabetes. Science 306: 457-461, 2004.
19. Zhang K and Kaufman RJ: The unfolded protein response: A stress signaling pathway critical for health and disease. Neurology 66 (2 Suppl 1): S102-S109, 2006.
20. Oakes SA and Papa FR: The role of endoplasmic reticulum stress in human pathology. Annu Rev Pathol 10: 173-194, 2015.
21. Gregor MF, Yang L, Fabbrini E, Mohammed BS, Eagon JC, Hotamisligil GS and Klein S: Endoplasmic reticulum stress is reduced in tissues of obese subjects after weight loss. Diabetes 58: 693-700, 2009.
22. Hillary RF and FitzGerald U: A lifetime of stress: ATF6 in development and homeostasis. J Biomed Sci 25: 48, 2018.
23. Klop B, Elte JW and Cabezas MC: Dyslipidemia in obesity: Mechanisms and potential targets. Nutrients 5: 1218-1240, 2013.
24. Engin A: Fat cell and fatty acid turnover in obesity. Adv Exp Med Biol 960: 135-160, 2017.
25. Tinahones FJ, Pareja A, Soriguer FJ, Gomez-Zumaquero JM, Cardona F and Rojo-Martinez G: Dietary fatty acids modify insulin secretion of rat pancreatic islet cells in vitro. J Endocrinol Invest 25: 436-441, 2002.

26. Sargsyan E, Artemenko K, Manukyan L, Bergquist J and Bergsten P: Oleate protects beta-cells from the toxic effect of palmitate by activating pro-survival pathways of the ER stress response. Biochim Biophysica Acta 1861: 1151-1160, 2016.
27. Karaskov E, Scott C, Zhang L, Teodoro T, Ravazzola M and Volchuk A: Chronic palmitate but not oleate exposure induces endoplasmic reticulum stress, which may contribute to INS-1 pancreatic beta-cell apoptosis. Endocrinology 147: 3398-3407, 2006.
28. Mayer CM and Belsham DD: Palmitate attenuates insulin signaling and induces endoplasmic reticulum stress and apoptosis in hypothalamic neurons: Rescue of resistance and apoptosis through adenosine 5' monophosphate-activated protein kinase activation. Endocrinology 151: 576-585, 2010.
29. Hall E, Volkov P, Dayeh T, Bacos K, Rönn T, Nitert MD and Ling C: Effects of palmitate on genome-wide mRNA expression and DNA methylation patterns in human pancreatic islets. BMC Med 12: 103, 2014.
30. Poitout V, Olson LK and Robertson RP: Insulin-secreting cell lines: Classification, characteristics and potential applications. Diabetes Metab 22: 7-14, 1996.
31. Assimacopoulos-Jeannet F, Thumelin S, Roche E, Esser V, McGarry JD and Prentki M: Fatty acids rapidly induce the carnitine palmitoyltransferase I gene in the pancreatic b-Cell line INS-1. J Biol Chem 272: 1659-1664, 1997.
32. Quinault A, Gausseres B, Bailbe D, Chebbah N, Portha B, Movassat J and Tourrel-Cuzin C: Disrupted dynamics of F-actin and insulin granule fusion in INS-1 832/13 beta-cells exposed to glucotoxicity: Partial restoration by glucagon-like peptide 1. Biochim Biophys Acta 1862: 1401-1411, 2016.
33. Kwon MJ, Chung HS, Yoon CS, Lee EJ, Kim TK, Lee SH, Ko KS, Rhee BD, Kim MK and Park JH: Low glibenclamide concentrations affect endoplasmic reticulum stress in INS-1 cells under glucotoxic or glucolipotoxic conditions. Korean J Intern Med 28: 339-346, 2013.
34. Seo HY, Kim YD, Lee KM, Min AK, Kim MK, Kim HS, Won KC, Park JY, Lee KU, Choi HS, *et al*: Endoplasmic reticulum stress-induced activation of activating transcription factor 6 decreases insulin gene expression via up-regulation of orphan nuclear receptor small heterodimer partner. Endocrinology 149: 3832-2841, 2008.
35. Walter P and Ron D: The unfolded protein response: From stress pathway to homeostatic regulation. Science 334: 1081-1086, 2011.
36. Sano R and Reed JC: ER stress-induced cell death mechanisms. Biochim Biophys Acta 1833: 3460-3470, 2013.
37. Hong SW, Lee J, Cho JH, Kwon H, Park SE, Rhee EJ, Park CY, Oh KW, Park SW and Lee WY: Pioglitazone attenuates palmitate-induced inflammation and endoplasmic reticulum stress in pancreatic β-Cells. Endocrinol Metab (Seoul) 33: 105-113, 2018.